

# Simulation and optimization of 2.6–2.8 $\mu\text{m}$ GaSb-based VCSELs

Łukasz Piskorski<sup>1</sup>  · Magdalena Marciniak<sup>1</sup> ·  
Jarosław Walczak<sup>1,2</sup>

Received: 30 August 2016 / Accepted: 18 April 2017 / Published online: 5 May 2017  
© The Author(s) 2017. This article is an open access publication

**Abstract** We present the simulation results of threshold operation of mid-infrared GaSb-based vertical-cavity surface-emitting lasers (VCSELs) obtained with the use of comprehensive fully self-consistent optical-electrical-thermal-recombination numerical model. The results show that by a proper design of VCSEL structure and composition of the active region it is theoretically possible to achieve room-temperature (RT) threshold operation for wavelength of 2.8  $\mu\text{m}$  which is about 0.2  $\mu\text{m}$  longer than those reported so far in the literature for III-V VCSELs with type-I quantum wells. Calculated values of the RT threshold current were equal to 2.5 and 4.0 mA for tunnel-junction diameters of 2 and 4  $\mu\text{m}$ , respectively.

**Keywords** VCSELs · Semiconductor devices · GaInAsSb · Mid-infrared range · Computer simulation

## 1 Introduction

Mid-infrared vertical-cavity surface-emitting lasers (VCSELs) have a great potential as low cost, ultra-low threshold, small beam divergence light sources in distant air monitoring. Although there are several important gases, like  $\text{C}_2\text{O}$ ,  $\text{N}_2\text{O}$ ,  $\text{H}_2\text{S}$ ,  $\text{CH}_4$  in the mid-infrared spectral range, the longest wavelength reported to date for electrically pumped room-temperature (RT) continues-wave (CW) VCSELs is 2.62  $\mu\text{m}$  (Arafin 2010). In this work we present the results of numerical analysis carried out for devices designed to emit

---

This article is part of the Topical Collection on Numerical Simulation of Optoelectronic Devices 2016.

Guest edited by Yuh-Renn Wu, Weida Hu, Sławomir Sujecki, Silvano Donati, Matthias Auf der Maur and Mohamed Swillam.

---

✉ Łukasz Piskorski  
lukasz.piskorski@p.lodz.pl

<sup>1</sup> Photonics Group, Institute of Physics, Lodz University of Technology, Wolczanska 219, 90-924 Lodz, Poland

<sup>2</sup> JWS, Piotrkowska 204/210/115, 90-924 Lodz, Poland

the light from the 2.6–2.8  $\mu\text{m}$  wavelength range. Due to the fact that the single-fundamental-mode operation is particularly suitable for absorption spectroscopy, we concentrate on suppression of the higher-order transverse modes in the modelled devices.

## 2 The laser structure

The structure under consideration was the GaSb-based quantum-well (QW) GaInAsSb/GaSb VCSEL (Fig. 1) similar to the device proposed in (Arafin 2009). Its intentionally undoped active region is assumed to be composed of 8-nm  $\text{Ga}_{1-x}\text{In}_x\text{As}_{0.15}\text{Sb}_{0.85}$  QWs (indium content  $x$  is equal to 0.43 and 0.49 for 1.6% and 2.0% compressively strained QWs, respectively) separated by 10-nm GaSb barriers. The active region is embedded in  $\text{Al}_{0.15}\text{Ga}_{0.85}\text{As}_{0.01}\text{Sb}_{0.99}$  waveguide and sandwiched by p- and n-type GaSb spacers. Above p-type spacer, the tunnel junction (TJ) composed of  $\text{p}^{++}\text{-GaSb}$  and  $\text{n}^{++}\text{-InAs}_{0.91}\text{Sb}_{0.09}$  is located. To minimize the absorption loss, the TJ is situated at the standing-wave node. Upper spacer is manufactured from n-GaSb. The  $3\text{-}\lambda$  cavity with several  $\text{n}^+\text{-GaSb}$  current spreading layers situated in cavity nodes is terminated on both sides by distributed-Bragg-reflectors (DBRs): the 4-pair  $\alpha\text{-Si/SiO}_2$  top DBR and the 24-pair  $\text{AlAs}_{0.08}\text{Sb}_{0.92}/\text{GaSb}$  bottom n-type DBR. Bottom DBR diameter is assumed to be equal to 100  $\mu\text{m}$ , whereas the upper DBR diameter is larger by 10  $\mu\text{m}$  than TJ diameter. The top contact is produced in a form of a ring of 5  $\mu\text{m}$  width. It is separated from the top spacer with the 200-nm thick highly-doped  $\text{n}^+\text{-InAs}_{0.91}\text{Sb}_{0.09}$  contact layer. The whole bottom 100- $\mu\text{m}$  diameter surface of the n-type GaSb substrate is covered by the bottom contact.

## 3 The model

Our three-dimensional optical-electrical-thermal-gain self-consistent VCSEL threshold-model has been adapted to simulate the CW operation of the GaSb-based VCSELs. The detailed description of the numerical algorithm applied in our model can be found in

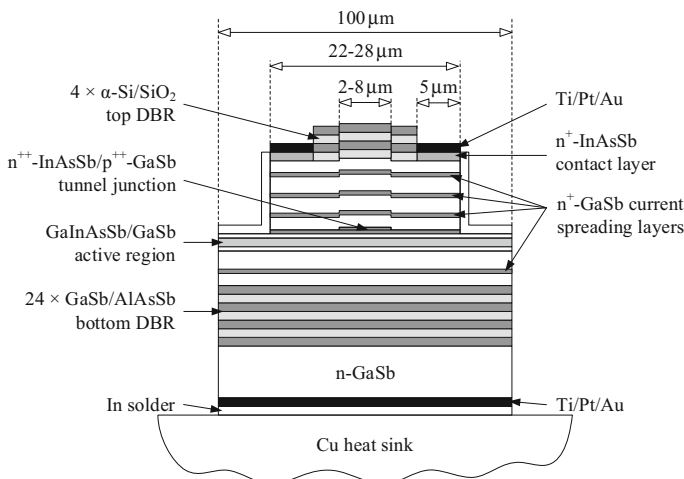


**Fig. 1** The structure of the modelled GaSb-based VCSELs. Not to scale

(Sarzala 2012), whereas in (Piskorski 2015) the method to calculate the shifts in the conduction and valence bands due to strain effects is presented. Values of all necessary material parameters can be obtained with the use of formulas given in (Piskorski 2016).

## 4 The results

As a verification of correctness of the set of material data we compared the experimental and numerical results for the voltage-current characteristics (Figs. 2a and 3a) and ambient temperature dependences of the threshold current (Figs. 2b and 3b) for two VCSELs emitting in the mid-infrared wavelength range. The first structure with the emission wavelength of 2.4- $\mu\text{m}$  was proposed in (Bachmann 2009), whereas the second one with the emission wavelength of 2.6- $\mu\text{m}$  in (Arafin 2009). The TJ diameters were equal to 6  $\mu\text{m}$  and 5.5  $\mu\text{m}$ , respectively. The main difference between these two VCSELs is the composition of the active region. In the 2.4- $\mu\text{m}$  device barriers are made from AlGaAsSb, whereas in the 2.6- $\mu\text{m}$  laser GaSb material is used in order to increase the valence band offset.

As can be seen in Figs. 2a and 3a, there is a very good agreement between experimental data for the voltage-current characteristics and theoretical results obtained with the use of our model. From that we can conclude that the electrical parameters (electrical conductivities, mobilities, free carrier concentrations) and the thermal conductivities have been correctly estimated. A slightly poorer agreement has been found for the ambient temperature dependences of the threshold current (Figs. 2b and 3b). However, the general trends are similar. The observed discrepancy can take its origin from the fact that in the real structure QWs might have slightly different material compositions and widths, whereas, in the simulation, they were identical to simplify the calculations. Moreover, we assumed that the carrier concentration is the same in every QW, which is not true in the real device. Both simplifications lead to broadening of the gain spectrum, and therefore have an influence on the ambient temperature dependences of the threshold current. Nevertheless, the gain and optical parameters seem to have reasonable values to perform the simulation of a device based on the antimonides.

In the above calculations five parameters were adjusted to fit the experimental data: (1) reverse saturation current density  $j_s = 1.0 \text{ A/m}^2$  and (2) shape factor  $\beta_{\text{pn}} = 40 \text{ V}^{-1}$

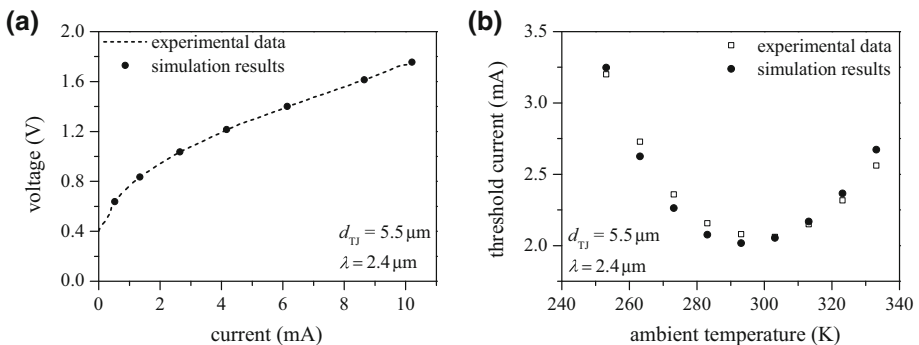


**Fig. 2** Comparison between experimental and numerical results for the: **a** voltage-current characteristics and **b** ambient temperature dependences of the threshold current for 2.4- $\mu\text{m}$  GaInAsSb/AlGaAsSb VCSEL with the 5.5- $\mu\text{m}$  TJ

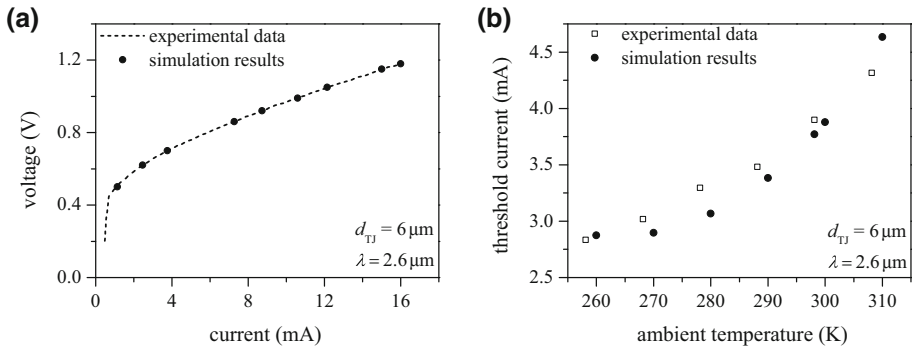


**Fig. 3** Comparison between experimental and numerical results for the: **a** voltage-current characteristics and **b** ambient temperature dependences of the threshold current for 2.6- $\mu\text{m}$  GaInAsSb/GaSb VCSEL with the 6- $\mu\text{m}$  TJ

from the classical diode equation (Piskorski 2011) which are necessary to find the effective conductivity of the active-region (Sarzała 2012), (3) effective electrical conductivity of the tunnel junction  $\sigma_{TJ} = 5.5 (\Omega \cdot \text{m})^{-1}$ , (4) matrix element  $M = 14 m_0 \cdot \text{eV}$  from the relation used in gain calculations (Piskorski 2015), and (5) shift of the conduction-band edge  $\Delta E_{c,BS} = 30 \text{ meV}$  due to the blueshift. Although matrix element can be obtained with the use of the Kane model (Vurgaftman 2001), its theoretical value is underestimated compared to the experimentally determined one (Chuang 2009). Blueshift, however, is the effect of annealing-induced interdiffusion on the electronic structure during the growth of the active region (Dier 2005). Energy shift caused by the above interdiffusion depends on the growth conditions, and therefore, it is specific for the given structure.

In Fig. 4 we present the values of the threshold current  $I_{th}$  for various ambient temperatures  $T_{amb}$  calculated for 2.6- $\mu\text{m}$  VCSEL with the strain in the QW equal to  $\epsilon = -1.6\%$ . As can be seen, with the increase of the  $T_{amb}$  the threshold current increases for all considered TJ diameters. This behaviour can be explained with the use of Fig. 5 in which we present the gain spectra calculated for VCSELs designed to emit the light from the 2.6–2.8  $\mu\text{m}$  wavelength range. For the 2.6- $\mu\text{m}$  device the gain peak is shifted to a longer wavelength than the emission one. To achieve the threshold operation for higher  $T_{amb}$  it is necessary to obtain the similar value of gain in the active region (in our calculations the threshold gain slightly increases which is a result of temperature influence on absorption coefficients taken into account). However, for higher temperatures, gain

**Fig. 4** Calculated threshold current vs. ambient temperature for 2.6- $\mu\text{m}$  VCSEL with 1.6% compressively strained QWs. Filled and empty symbols correspond to LP<sub>01</sub> and LP<sub>11</sub> mode operation, respectively

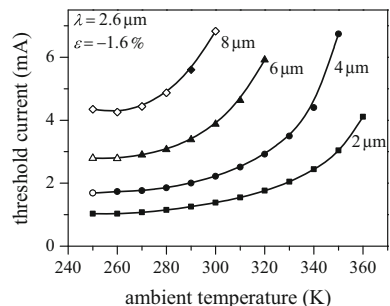
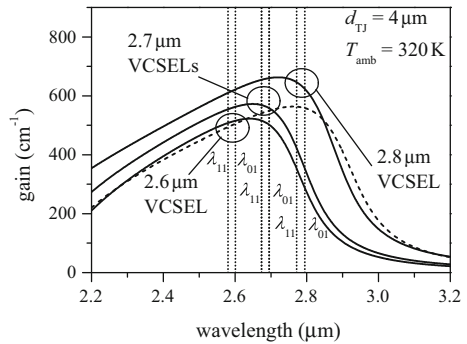


**Fig. 5** Gain spectra calculated for VCSELs with 4- $\mu\text{m}$  TJ diameter emitting in the 2.6–2.8  $\mu\text{m}$  wavelength range with 1.6% (solid lines) and 2.0% (dashed line) compressively strained QWs. Wavelengths corresponding to the LP<sub>01</sub> and LP<sub>11</sub> modes have been additionally shown



calculated for a fixed carrier concentration decreases. Therefore, it is necessary to increase the carrier concentration in the active region which leads to the higher  $I_{th}$ . From Fig. 4 it can be also seen that for wider apertures the temperature range, in which the LP<sub>01</sub> mode operation is achieved, decreases. This can be explained by the fact that for wider apertures the LP<sub>11</sub> mode losses calculated in respect to LP<sub>01</sub> mode become smaller.

For the device with the same active region but designed to emit the wavelength of 2.7  $\mu\text{m}$  by increasing the thickness of DBR layers and the optical length of the cavity, we obtained the stable LP<sub>01</sub> mode operation only for the TJ with the smallest aperture (Fig. 6a). As can be seen from Fig. 5, for 2.7- $\mu\text{m}$  VCSEL and  $\epsilon = -1.6\%$ , due to the shift of gain spectrum towards the longer wavelengths, the value of gain for the wavelength corresponding to LP<sub>11</sub> mode is higher than the one for LP<sub>01</sub> mode. This leads to the significant reduction of the LP<sub>11</sub> mode losses, and therefore we observe LP<sub>11</sub> mode operation for all considered apertures wider than 2  $\mu\text{m}$ , for which the LP<sub>11</sub> mode losses are still enough high to provide LP<sub>01</sub> mode emission. We performed analogous calculations for 2.8- $\mu\text{m}$  VCSEL with the strain in the QW equal to  $\epsilon = -1.6\%$ . For this device LP<sub>11</sub> mode operation is more favourable than for the 2.7- $\mu\text{m}$  VCSEL with the same active region. The

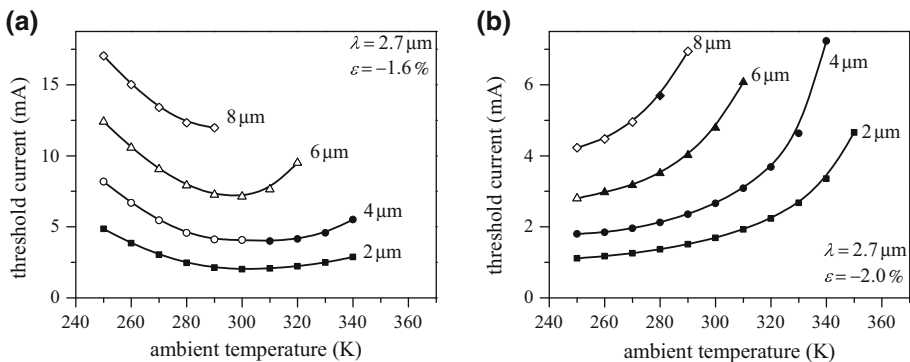


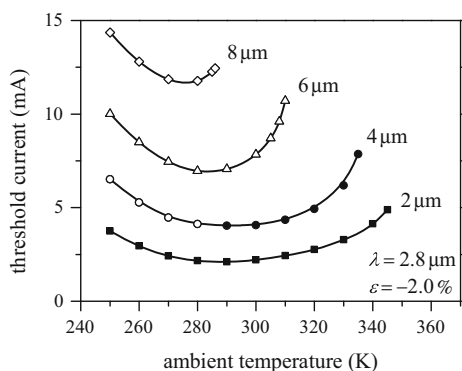
**Fig. 6** Calculated threshold current vs. ambient temperature for 2.7- $\mu\text{m}$  VCSEL with **a** 1.6% and **b** 2.0% compressively strained QWs. Filled and empty symbols correspond to LP<sub>01</sub> and LP<sub>11</sub> mode operation, respectively

values of the threshold current which, we do not report here, follow the same trend where the threshold current increases and the temperature range, for which LP<sub>01</sub> mode operation is observed, decreases. As a result, for the 2.8- $\mu\text{m}$  VCSEL, we obtained the stable fundamental mode operation only for device with TJ diameter of 2  $\mu\text{m}$

One of methods to increase the LP<sub>11</sub> mode losses and therefore to obtain laser operation in the LP<sub>01</sub> mode is to shift the gain spectrum toward the longer wavelength. In VCSELs, for the situation when the wavelength corresponding to the gain peak is longer than the emission wavelength, the LP<sub>01</sub> mode operation is more favourable than the LP<sub>11</sub> one. In our calculations we shifted the gain spectrum for the 2.7- $\mu\text{m}$  VCSEL (Fig. 5) by increasing the indium content in the GaInAsSb QWs from 0.43 to 0.49 which was followed by the increase in the value of compressive strain by 0.4%. As a result we obtained the stable LP<sub>01</sub> mode operation for TJ diameters up to 6  $\mu\text{m}$  (Fig. 6b) with the distinctly lower values of the threshold currents. Although the compressive strain of 1.6% in our initial structure is high, surface-emitting lasers with antimonide-based active regions with even higher strain in QWs were already reported. In (Rösener 2011) the solid-source molecular beam epitaxy was used to grow active region which consists of ten compressively strained GaInAsSb QWs for whose the compressive strain was determined to be of 1.8% with the use of high-resolution x-ray diffraction. Higher strain (2.08%) for active region with ten GaInAsSb QWs was reported in (Holl 2016), where it is also mentioned that the thickness of each QW was equal to 10 nm. It is the same value which we used in calculations described in this paper. Although the higher strain leads to a reduction of the critical thickness at which relaxation of the QW layers occurs, it seems that active regions considered here can be realized with the use of present technology.

The structure with the 2% compressively-strained active-region was further modified in order to achieve emission around 2.8  $\mu\text{m}$ . Similarly to the 2.7- $\mu\text{m}$  devices, the thickness of DBR layers and n-GaSb layers in the cavity have been increased. As can be seen from Fig. 7 after the above modifications we obtained LP<sub>01</sub> mode operation above RT for TJ diameters up to 4  $\mu\text{m}$ . Calculated values of the RT threshold current were equal to 2.5 and 4.0 mA for tunnel-junction diameters of 2 and 4  $\mu\text{m}$ , respectively. The threshold current values and temperature-operation ranges for the corresponding TJ diameters are similar to those from Fig. 6a which is the result of the similar cavity-gain detuning for these lasers.

**Fig. 7** Calculated threshold current vs. ambient temperature for 2.8- $\mu\text{m}$  VCSEL with 2.0% compressively strained QWs. Filled and empty symbols correspond to LP<sub>01</sub> and LP<sub>11</sub> mode operation, respectively



## 5 Conclusion

We performed the threshold analysis of an operation of GaSb-based VCSELs emitting in the 2.6–2.8  $\mu\text{m}$  wavelength range. The simulation was performed for VCSELs with various TJ diameters and for ambient temperatures ranging from 250 K to the maximal operating temperature for a given device. The results show that by a proper design of VCSEL structure and composition of the active region it is theoretically possible to achieve the threshold operation for wavelengths about 0.2  $\mu\text{m}$  longer than those reported so far in the literature. Moreover, obtaining the desired low-threshold stable single-fundamental-mode operation in these devices is also possible.

Our results may be useful for designing the electrically-pumped continuous-wave III-V VCSELs able to achieve the emission wavelength of 3  $\mu\text{m}$ .

**Acknowledgements** This work has been supported by the Polish National Science Centre (DEC-2012/07/D/ST7/02581).

**Open Access** This article is distributed under the terms of the Creative Commons Attribution 4.0 International License (<http://creativecommons.org/licenses/by/4.0/>), which permits unrestricted use, distribution, and reproduction in any medium, provided you give appropriate credit to the original author(s) and the source, provide a link to the Creative Commons license, and indicate if changes were made.

## References

- Arafin, S., Bachmann, A., Kashani-Shirazi, K., Amann, M.-C.: Continuous-wave electrically-pumped GaSb-based VCSELs at 2.6  $\mu\text{m}$  operating up to 50 °C. In: Proceeding of the 22nd Annual Meeting of the IEEE Photonics Society, p. 837 (2009)
- Arafin, S., Bachmann, A., Vizbaras, K., Amann, M.-C.: Large-aperture single-mode GaSb-based BTJ-VCSELs at 2.62  $\mu\text{m}$ . In: Proceeding of the 22nd IEEE International Semiconductor Laser Conference, p. 47 (2010)
- Bachmann, A., Arafin, S., Kashani-Shirazi, K.: Single-mode electrically pumped GaSb-based VCSELs emitting continuous-wave at 2.4 and 2.6  $\mu\text{m}$ . *New J. Phys.* **11**, 125014-1–125014-17 (2009)
- Chuang, S.L.: *Physics of Photonic Devices*. Wiley, Hoboken (2009)
- Dier, O., Dachs, S., Grau, M., Chun, L., Lauer, C., Amann, M.-C.: Effects of thermal annealing on the band gap of GaInAsSb. *Appl. Phys. A* **86**, 151120-1–151120-3 (2005)
- Holl, P., Rattunde, M., Adler, S., Bächle, A., Diwo-Emmer, E., Aidam, R., Manz, C., Köhler, K., Wagner, J.: Optimization of 2.5  $\mu\text{m}$  VECSEL: influence of the QW active region, in *Vertical External Cavity Surface Emitting Lasers (VECSELs) VI*, Wilcox K.G. (ed.), In: Proceeding of SPIE **9734**, p. 97340S (2016)
- Piskorski, Ł., Sarzała, R.P., Nakwaski, W.: Investigation of temperature characteristics of modern InAsP/InGaAsP multi-quantum-well TJ-VCSELs for optical fibre communication. *Opto-Electron. Rev.* **19**, 320–326 (2011)
- Piskorski, Ł., Frasunkiewicz, L., Sarzała, R.P.: Comparative analysis of GaAs- and GaSb-based active regions. *Bull. Pol. Acad. Tech.* **63**, 597–603 (2015)
- Piskorski, Ł., Sarzała, R.P.: Material parameters of antimonides and amorphous materials for modelling the mid-infrared lasers. *Opt. Appl.* **46**, 227–240 (2016)
- Rösener, B., Rattunde, M., Moser, R., Kaspar, S., Töpfer, T., Manz, Ch., Köhler, K., Wagner, J.: Continuous-wave room-temperature operation of a 2.8  $\mu\text{m}$  GaSb-based semiconductor disk laser. *Opt. Lett.* **36**, 319–321 (2011)
- Sarzała, R.P., Czystanowski, T., Wasiak, M., Dems, M., Piskorski, Ł., Nakwaski, W., Panajotov, K.: Numerical self-consistent analysis of VCSELs. *Adv. Opt. Technol.* **2012**, 689519-1–689519-17 (2012)
- Vurgaftman, I., Meyer, J.R., Ram-Mohan, L.R.: Band parameters for III-V compound semiconductors and their alloys. *J. Appl. Phys.* **89**, 5815–5875 (2001)